Mode expansion and Bragg filtering enable a high-fidelity fiber-based photon-pair source

Alexander Ling*, Jun Chen, Jingyun Fan and Alan Migdall

National Institute of Standards and Technology, Gaithersburg, MD 20899
Joint Quantum Institute, University of Maryland, College Park, MD 20742

*aling@nist.gov

Abstract: We report the development of a fiber-based single spatial mode source of photon-pairs where the efficiency of extracting photon-pairs is 14× better than a previous implementation [16]. This critical improvement in efficiency enabled a spectrally bright and pure photon-pair source having a small second-order correlation function (0.03) and a raw spectral brightness of 44,700 pairs $s^{-1}nm^{-1}mW^{-1}$. The source can be configured to generate entangled photon-pairs, characterized via optimal and minimal quantum state tomography, to have a fidelity of 97% and tangle of 92%, without subtracting any background.

References and links

[1] D. C. Burnham and D. L. Weinberg, Phys. Rev. Lett. **25**, 84 (1970) .
[2] C. Kurtsiefer, M. Oberparleiter, and H. Weinfurter, Phys. Rev. A **64**, 023802 (2001).
[3] A. Fedrizzi, T. Herbst, A. Poppe, T. Jennewein, and A. Zeilinger, Opt. Express **15**, 15377 (2007).
[4] A. B. U'Ren, C. Silberhorn, K. Banaszek, and I. A. Walmsley, Phys. Rev. Lett. **93**, 093601 (2004).
[5] M. Fiorentino, S. M. Spillane, R. G. Beausoleil, T. D. Roberts, P. Battle, and M. W. Munro, Opt. Express **15**, 7479 (2007).
[6] J. Chen, A. J. Pearlman, A. Ling, J. Fan, and A. Migdall, Opt. Express **17**, 6727 (2009).
[7] A. Christ, K. Laiho, A. Eckstein, T. Lauckner, P. J. Mosley, and C. Silberhorn, arXiv:0904.4668v1 (2009).
[8] M. Karpinski, C. Radzewicz, and K. Banaszek, arXiv:0904.4577v1 (2009).
[9] J. Fan, A. Migdall, and L. J. Wang, Opt. Lett. **30**, 3368 (2005).
[10] H. Takesue and K. Inoue, Opt. Express **13**, 7832 (2005).
[11] J. Chen, K. F. Lee, C. Liang, and P. Kumar, Opt. Lett. **31**, 2798 (2006).
[12] K. F. Lee, J. Chen, C. Liang, X. Li, P. L. Voss, and P. Kumar, Opt. Lett. **31**, 1905 (2006).
[13] P. Russell, Science **299**, 358 (2003).
[14] J. Fan, M. D. Eisaman, and A. Migdall, Phy. Rev. A **76**, 043836 (2007).
[15] E. A. Goldschmidt, M. D. Eisaman, J. Fan, S. V. Polyakov, and A. Migdall, Phys. Rev. A **78**, 013844 (2008).
[16] J. Fulconis, O. Alibart, J. L. O'Brien, W. J. Wadsworth, and J. G. Rarity, Phys. Rev. Lett. **99**, 120501 (2007).
[17] J. Chen, X. Li, and P. Kumar, Phys. Rev. A **72**, 033801 (2005).
[18] J. Fan and A. Migdall, Opt. Express **15**, 2915 (2007).
[19] S. Jobling, K. T. McCusker, and P. G. Kwiat, in *Poster JWA32, Frontiers in Optics* (2008).
[20] R. Loudon, *The Quantum Theory of Light* (New York:Oxford University Press, 1983).
[21] S. Fasel, O. Alibart, S. Tanzilli, P. Baldi, A. Beveratos, N. Gisin, and H. Zbinden, New Journal of Physics **6**, 63 (2004).
[22] URL `http://www.nist.gov/fpga`.
[23] J. Řeháček, B.-G. Englert, and D. Kaszlikowski, Phys. Rev. A **70**, 052321 (2004).
[24] A. Ambirajan and D. C. Look, Opt. Eng. **34**, (6), 1651 (1995).
[25] A. Ambirajan and D. C. Look, Opt. Eng. **34**, (6), 1656 (1995).
[26] E. Hecht, *Optics, 4th Edition* (Addison Wesley, 2002).
[27] A. Ling, K. P. Soh, A. Lamas-Linares, and C. Kurtsiefer, Journal of Modern Optics **56**, 1523 (2006a).
[28] A. Ling, K. P. Soh, A. Lamas-Linares, and C. Kurtsiefer, Phys. Rev. A **74**, 022309 (2006b).
[29] J.-W. Pan, D. Bouwmeester, H. Weinfurter, and A. Zeilinger, Phys. Rev. Lett. **80**, 3891 (1998).

[30] C. K. Hong, Z. Y. Ou, and L. Mandel, Phys. Rev. Lett. **59**, 2044 (1987).
[31] H. de Riedmatten, I. Marcikic, J. A. W. van Howelingen, W. Tittel, H. Zbinden, and N. Gisin, Phys. Rev. A **71** (2005).
[32] H. d. Riedmatten, I. Marcikic, W. Tittel, H. Zbinden, and N. Gisin, Phys. Rev. A **67**, 022301 (2003).,
[34] O. Cohen, J.S. Lundeen, B. J. Smith, G. Puentes, P. J. Mosley, and I. A. Walmsley, arXiv:0809.0071v2 (2008)
[33] K. Garay-Palmett, H. J. McGuinness, O. Cohen, J. S. Lundeen, R. Rangel-Rojo, A. B. U'ren, M. G. Raymer, C. J. McKinstrie, S. Radic, and I. A. Walmsley, Opt. Express **15**, 14870 (2007).
[36] J. Heersink, V. Josse, G. Leuchs, and U. L. Andersen, Opt. Lett. **30**, 1192 (2005).
[37] J. Milanovic, M. Lassen, U. L. Andersen, and G. Leuchs, arXiv:0902.4597v1 (2009).
[35] M. Halder, J. Fulconis, B. Cemlyn, A. Clark, C. Xiong, W. J. Wadsworth, and J. G. Rarity, Opt. Express **17**, 4670 (2009).

1. Introduction

The contemporary workhorse method for obtaining photon-pairs has been Spontaneous Parametric Down Conversion (SPDC) [1] in nonlinear crystals. Typical SPDC sources employ bulk crystals whose output is coupled into single-mode fibers [2, 3]. However, because SPDC emission from bulk crystals is inherently spatially multi-mode, only a fraction of the two-photon yield can be collected into a single-mode fiber. This is one reason that has prompted numerous studies on SPDC inside waveguides [4, 5, 6, 7, 8], as the overlap of the total emitted light with a single spatial mode is much better in this regime.

Another approach, which is the subject of this paper, is to generate photon-pairs via Spontaneous Four-Wave Mixing (SFWM) inside optical fibers [9, 10, 11, 12]. Of particular interest is SFWM inside of a solid core photonic crystal fiber [13] (PCF), which has spatial mode sizes typically an order of magnitude smaller than in conventional fibers, resulting in much higher nonlinearity. Combined with appropriate phase-matching conditions, SFWM in PCFs has enabled very bright polarization-entangled photon-pair sources (even after aggressive spectral filtering) operating at room temperature [14]. However, the PCF source still has outstanding issues. Most significantly, the performance of PCF sources suffer from low extraction efficiency; losses are typically high when the pairs are to be prepared into a well-defined bandwidth with a useful single spatial mode.

In this paper we report an improvement of $14\times$ for the extraction efficiency, compared to earlier implementations of PCF sources [15, 16]. This was enabled by incorporating several novel (and simple-to-use) elements, including end-tapered PCFs, high efficiency reflection Bragg gratings and high transmission band-pass filters. On this basis the quality and spectral brightness of single-mode photon-pair SFWM sources are significantly improved. The photon-pair purity of the source, determined using the second order correlation function ($g^{(2)}(0)$), was measured to be as small as 0.0055. When the source is used to generate polarization-entangled photon-pairs, the fidelity (to a Bell state) and tangle are measured to be 97% and 92% respectively. Indistinguishable photons have also been heralded by detection of their twins, which exhibit a high level of indistinguishability via the demonstration of a 82% raw visibility Hong-Ou-Mandel interference dip.

2. Photon-pair purity

To simplify the discussion, and as the basic theory of SFWM inside fibers has been well described previously [17], we begin by describing our experimental parameters.

2.1. Efficient extraction of photon-pairs

In our photon-counting experiments (fig. 1), we work with PCFs engineered to be polarization maintaining along two principal axes. To maximize the nonlinear gain, the pump polarization

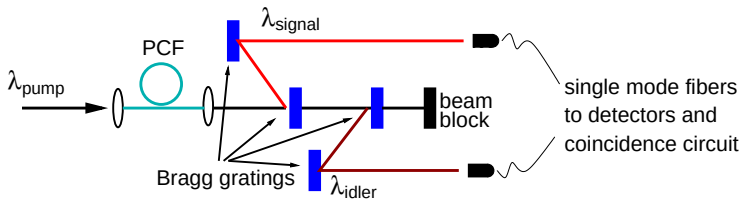

Fig. 1. (Color online) Layout of first experiment for pumping a PCF and collecting photon-pairs. Photon-pairs are detected via a start-stop coincidence circuit. Reflection Bragg gratings separate signal and idler from the pump. Using two gratings per arm suppresses the pump light by up to 180 dB.

is aligned with the axis which exhibits higher nonlinearity; this configuration also enables the generation of co-polarized photon-pairs.

The PCF we use has a length of one meter and a nominal zero dispersion wavelength of 745 ± 5 nm. The core diameter of the PCF is $\approx 1\mu$m, but the diameter at the ends were expanded to 15 μm by collapsing the fiber structure over a length of 50 μm. To reduce the influence of uncorrelated single photons due to Raman Scattering, the pump wavelength is tuned to 741.7 nm, which is slightly blue-detuned compared to the zero-dispersion wavelength [18, 16]. This improves photon-pair purity without much loss in the pair production rate.

The pump is a pulsed Ti:Sapphire laser (repetition rate of 76 MHz, and pulse duration of 8 ps). Phase matching results in the peak of the signal and idler wavelengths being at 690.4 and 801.2 nm respectively. After spectral filtering, photons are collected into single-mode fibers and detected by Si avalanche photo-diodes (APDs). Electronic signals from the detectors are sent to a start-stop data acquisition system for coincidence monitoring (5 ns time window).

The ends of the PCF are not anti-reflection coated resulting in a emission efficiency of $\eta_{fiber} = 96\%$. The collapsed fiber ends, with their resulting larger optical modes, allow the use of simple and inexpensive aspheric lenses (NA=0.25, measured transmission efficiency $\eta_{lens} = 98\%$) to couple light into and out of the fiber, rather than high-magnification microscope objectives [15, 18]. To select the photons in the signal and idler channels within a narrow spectral bandwidth, and to reject the pump, reflection Bragg gratings are used (two gratings per channel). The measured suppression of the pump with a single grating is ≈ 90 dB, giving a combined suppression of 180 dB. Typical pump power is ≈ 1 mW; at this level the combined suppression results in a negligible pump presence at the APDs compared to the photon-pair count rates of several thousand per second.

The full-width-at-half-maximum (FWHM) for the signal filter is of 0.17 nm and to maximize the collection of all correlated photons, the bandwidth for idler photons must be at least 0.23 nm. To meet this requirement and to allow for a 0.1 nm pump bandwidth, the idler filter bandwidth is fixed at 0.3 nm. The measured peak grating reflectance is larger than 98%. However, the photon-pairs are carved from a broad SFWM spectrum, and (conservatively) assuming that the filters have a Gaussian band-pass profile, the average grating efficiency, $\eta_{grating}$, is 87%. Using two gratings in reflectance leads to a combined efficiency of $\eta^2_{grating} = 76\%$. All transmitted light suffer $\approx 10\%$ scattering losses within the grating.

The single spatial mode is defined by the single-mode collection fibers. To maximize the detection rate of highly detuned photon-pairs, the fiber-coupling efficiencies, $\eta_{coupling}$, for the signal and idler wavelengths are matched at 50%. This efficiency should increase with the use of mode-matching optics such as cylindrical lenses or more sophisticated adaptive optics techniques that have demonstrated 97% coupling efficiency between single-mode fibers [19].

These values determine the single photon extraction efficiency. For signal photons, this is

Table 1. Extraction efficiencies for different PCF sources. Source [15] used grating-based spectrometers for spectral selection, while [16] used dichroic mirrors and bandpass filters. Photon-pair detection efficiency of the end-tapered source is 14 times larger than previously reported implementations [15, 16].

Efficiency (%)

	Our source		Source: [15]		Source: [16]	
	signal	idler	signal	idler	signal	idler
η_{fiber}	96	96	96	96	N.A.	
η_{lens}	98	98	75	70	N.A.	
spectral selection eff.	76	68	16	27	N.A.	
$\eta_{coupling}$	50	50	53	58	N.A.	
extraction eff.	36	32	6.1	11	N.A.	
η_{det}	60	50	60	50	N.A.	
Single Photon Detection Eff.	22	16	3.7	5.5	5.0	5.0
Photon-pair Detection Eff.	3.5		0.2		0.25	

$\eta_{signal} = \eta_{coupling}\eta^2_{grating}\eta_{lens}\eta_{fiber} = 36\%$, whereas for idler photons (which suffer the additional scattering loss) $\eta_{idler} = 0.9 \times \eta_{coupling}\eta^2_{grating}\eta_{lens}\eta_{fiber} = 32\%$. The overall photon-pair extraction efficiency is ($\eta_{signal}\eta_{idler} \approx$) 12%, which is higher than previous implementations that used microscope objectives [15], inferred to be 0.7% .

The single photon detectors have detection efficiencies, η_{det}, of 60% at 690.4 nm and 50% at 801.2 nm. The single photon detection efficiency for signal photons is 22% and for idler photons is 16%. The maximum coincidence-to-singles ratio (which is a gauge of single photon detection efficiency) is 10% due to the presence of uncorrelated single photons.

Putting all the efficiencies together, we find that in our single-mode pair source approximately 3.7% of all generated photon-pairs are detected. This is substantially higher than the collection efficiencies of previous implementations that achieved efficiencies of 0.25% [16] and 0.21% [15] respectively (Table 1).

2.2. Measured purity

Higher pair detection efficiency, together with the narrower selected bandwidth, enables a high purity photon-pair source. The photon-pair purity is important as it determines the background (caused by erroneously identified pairs) limiting the useful visibility in experiments. This purity can be estimated using either the coincidence-to-accidentals ratio (C/A), and from the second-order correlation function $g^{(2)}(0)$ [20]. C/A is commonly used [11, 12] because the accidentals rate is a direct estimate of the background level. The C/A parameters can be obtained directly from two-fold coincidence measurement setups such as the one in fig. 1.

To determine the C/A, it is necessary to estimate the rate of accidental coincidences. To a first approximation, the rate of coincidences between different pump pulses is a good estimate of the accidentals rate. Our start-stop acquisition system lets us monitor coincidence and accidental counts simultaneously. The observed C/A on pump power (and detected pair rate) for our PCF is shown in fig. 2 (a).

The second-order correlation function is a direct measure of the presence of multiple photons (per pulse) in the signal and idler channels. When there is only one pair per pulse, $g^{(2)}(0) = 0$; in practice this is never achieved because of detector dark counts. A semiclassical theory of light establishes a lower limit of 1 for the $g^{(2)}(0)$ of classical coherent light sources [20]. Thus we would expect that the $g^{(2)}(0)$ values for our source would lie somewhere between 0 and 1,

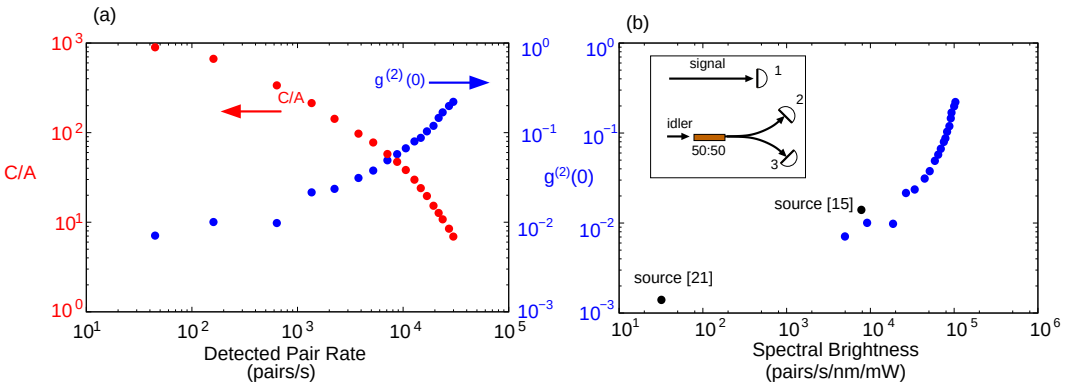

Fig. 2. (Color online) Two measures of photon-pair purity: the coincidence-to-accidentals ratio (C/A) and $g^{(2)}(0)$. (a) Photon-pair purity dependence on the detected pair rate. (b) $g^{(2)}(0)$ against *raw* spectral brightness. The inset indicates the detection arrangement for obtaining the $g^{(2)}(0)$. The signal photon acts as a herald, while the idler photons are sent into a polarization neutral 50:50 beamsplitter. The rate of three-fold and two-fold coincidences determine the value of $g^{(2)}(0)$.

when operated with low pump power.

In the measurement scheme for this (inset of fig. 2 (b)), the idler photons are incident on a 50:50 fiber beamsplitter whose output ports are sent to APDs. The detector in the signal arm acts as the herald for a three-fold coincidence. Following a simple model described in [21], the correlation function is

$$g^{(2)}(0) = \frac{4C_{123}C_1}{(C_{12}+C_{13})^2} \tag{1}$$

where the three-fold coincidence rate is C_{123}, the rate of signal photons is C_1, and the two-fold rate between signal and idler detectors are C_{12} and C_{13}, The three-fold coincidences were detected with an electronic circuit based on FPGA technology [22]. The measured correlation values (fig. 2) are much less than 1 signifying the nonclassical nature of the emitted light.

Figure 2 (a) links photon-pair purity with the detected pair rate. From the figure, a detection rate of 45 pairs s^{-1} (≈ 0.05 mW) has $g^{(2)}(0) = 0.007 \pm 0.005$, and a C/A = 900 (C/A $\rightarrow \infty$ for no background accidentals). When pump power is increased to 0.5 mW, the detected pair rate is 3,800 pairs s^{-1}, $g^{(2)}(0) = 0.03 \pm 0.001$ and C/A=100. For comparison, a very good photon-pair source based on SPDC [21] exhibits a $g^{(2)}(0)$ of 0.0014 ± 0.0003, with a count rate of 350 pairs

Table 2. Selected data points from fig. 2 (b) for comparing $g^{(2)}(0)$ values between different sources. Increasing the pump repetition rate, but keeping peak pulse power constant, it should be possible to increase the pair production rate while maintaining the level of $g^{(2)}(0)$.

	$g^{(2)}(0)$	Detected Rate (pairs s^{-1})	Bandwidth (nm)	Spectral Brightness (pairs $s^{-1}nm^{-1}mW^{-1}$)
Our Source	0.007 ± 0.005	45	0.17	5,300
	0.03 ± 0.001	3,800	0.17	44,700
Source [15]	0.014 ± 0.002	350	0.9	7,800
Source [21]	0.0014 ± 0.0003	350	6.9	32

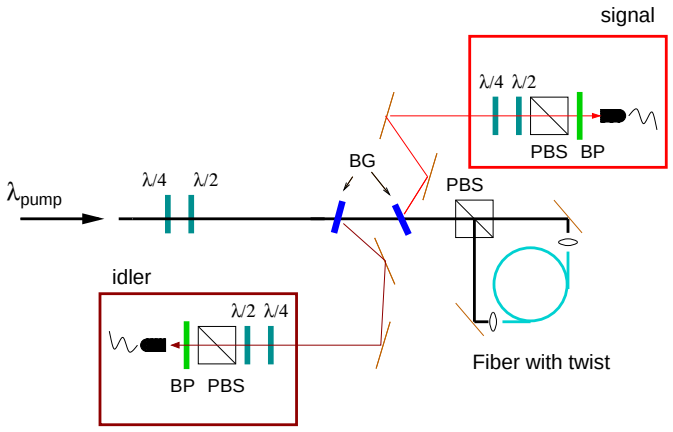

Fig. 3. (Color online) Schematic of the polarization-entangled photon-pair source based on a 90^o twist of the photonic crystal fiber. The PCF is pumped in both directions. A single Bragg grating (BG) selects for each of the signal and idler; to suppress residual pump light highly transmissive ($>$ 99%) bandpass (BP) filters are used. The entangled state is analyzed using a combination of quarter-wave ($\frac{\lambda}{4}$) and half-wave ($\frac{\lambda}{2}$) plates together with a polarizing beam splitter (PBS).

s^{-1} and bandwidth of 6.9 nm. To compare spectral brightness between sources, the pair rate is often normalized to pump power and collected bandwidth. After this normalization, the *raw* spectral brightness of our source (at 0.5 mW) is 44,700 pairs (s nm mW)$^{-1}$ (fig. 2 (b)). Selected points from fig. 2 (b) are presented in Table 2.

3. Polarization-entangled photon-pairs

Here, we characterize a polarization-entangled pair source built around an end-tapered PCF. This is done by using a coherent superposition of $|HH\rangle$ and $|VV\rangle$, where $|HH\rangle$ and $|VV\rangle$ represent the horizontal and vertical polarization states of photon-pairs. Such a superposition may be generated by placing the PCF in a Sagnac loop as reported in [14, 16] (fig. 3).

To generate the orthogonal polarization states, only one principal axis of the PCF is pumped from both ends. The axis at one end was aligned to match with the H output of a polarizing beam splitter (PBS). The PCF was twisted so that the axis orientation at the other end is matched with the V output of the PBS. The extinction ratio of a PCF-based Sagnac loop is better than 200:1. Light from the pulsed laser is split by the PBS and pumps the PCF in two directions. By controlling the polarization of the pump (and hence its splitting ratio at the PBS), it is possible to balance the pair production from both outputs of the PCF. This is necessary because the photon-pair production rates for the two pump directions are not equal (by $\approx$ 20%), despite having the same level of inserted pump power (most probably due to non-uniformity in the PCF).

The recombination of light from both ends at the PBS generates the superposition of $|HH\rangle$ and $|VV\rangle$, producing a polarization-entangled photon-pair state. Using only a single Bragg grating for each wavelength, we are able to separate the desired signal and idler photons from the rest of the light output. Sufficient suppression of pump light was achieved with the help of an additional bandpass filter. These filters are centered on 800 nm (FWHM $\approx$ 12 nm) and 692 nm (FWHM $\approx$ 40 nm) respectively, both having a measured transmission efficiency of 99% and a box-like spectral selection profile.

The polarization-entangled state can be completely characterized by quantum state tomog-

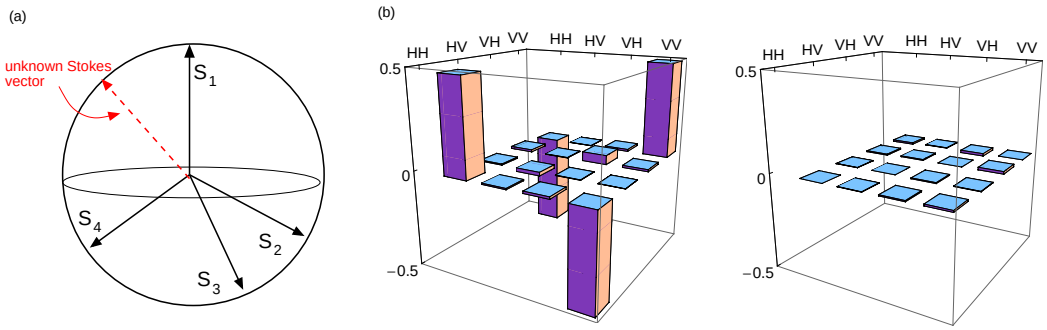

Fig. 4. (Color online) (a) illustrates the concept of minimal and optimal tomography for an unknown Stokes vector. (b) is a graphical representation of the density matrix obtained using minimal and optimal quantum state tomography. The real part of the matrix is on the left; the imaginary part is the right. The magnitude of the components in the imaginary part are less than 0.013. The fidelity to the Φ^- Bell state is $97 \pm 1\%$.

raphy. We used a tomographic technique that is known to be minimal and optimal [23]. The key point of this technique is that the polarization state of light is described by a Stokes vector which has only three independent variables [24, 25]. Such a Stokes vector can be illustrated on a Poincare sphere (fig. 4 (a)). The direction and magnitude of any Stokes vector is completely determined by its overlap with four other reference vectors in the sphere. In contrast, standard polarimetry requires six overlap measurements [26]. It was further shown that when these reference vectors define a tetrahedron in the Poincare sphere, the characterization rate is optimized [23]. Hence, characterization of single photon polarization states requires only 4 projective measurements [27]. This is of particular importance when considering N-photon states, where the number of projective measurements grows as 4^N [28], in contrast to standard polarimetry that grows as 6^N.

To characterize our photon-pair state, we needed to monitor 16 separate two-fold coincidences. This was done by projecting the signal photons sequentially onto the 4 reference polarizations states; the reference states were prepared by rotating the half-wave and quarter-wave plates (fig. 3) to the angles described in [25]. For each projection state of the signal, the idler photons are also projected onto the same four reference states. In this way, we obtain the 16 combinations of coincidences that are sufficient to obtain a photon-pair Stokes vector that can be converted into a density matrix [28].

The source is typically operated at room temperature with a pump power of 1 mW (before the PBS), and the detected pair rate is $\approx 2,800 \mathrm{s}^{-1}$. The detected rate is lower than with a single pump direction setup because the spatial mode shapes from the two fiber ends are slightly different, causing additional loss in coupling into single-mode fibers that define the useful spatial mode as well as transmit light to the APDs. The density matrix of our photon-pair state (at 1 mW of pump power and *without* correcting for accidentals) is reconstructed and shown in fig. 4 (b). The fidelity of this density matrix to the maximally entangled Bell state, $\Phi^- = \frac{1}{\sqrt{2}}(|\mathrm{HH}\rangle - |\mathrm{VV}\rangle)$, is $97 \pm 1\%$ (error propagation assumes a Poissonian noise model and standard error propagation is used). The tangle is one method of quantifying the degree of entanglement, and from our measured density matrix the tangle is found to be $92 \pm 2\%$.

4. Heralded indistinguishable single photons

Another possible use of the end-tapered PCF is to act as a source of heralded indistinguishable single photons. We note that a single PCF that is pumped bi-directionally acts effectively as

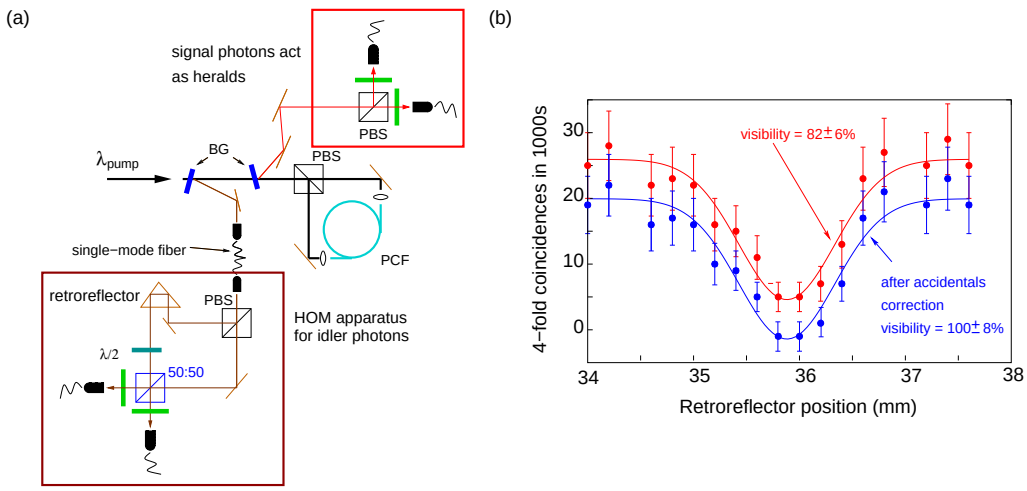

Fig. 5. (Color online) (a) Scheme for measurement of the Hong-Ou-Mandel Interference dip. The signal photons act as heralds for the idler photons. For interference to take place, the idler photons are all set to the H polarization. (b) The observed HOM dip at approximately 1 mW of pump power in each arm of the PCF. When corrected for accidentals, the HOM dip is compatible with unit visibility.

two sources of heralded single photons (similar to some SPDC experiments where a nonlinear crystal is pumped in two directions [29]). When combined with the spectral filtering described in previous sections, the idler (and signal) photons generated from either end of a PCF are effectively indistinguishable. We demonstrate this feature by performing the classic Hong-Ou-Mandel (HOM) photon interference experiment [30].

This experiment (fig. 5(a)) is a modification of the setup that was used to generate the polarization-entangled pairs. Here two pairs of photons were collected, one pair from each output of the PCF. Using the FPGA-based counting system, the overall rate of four-fold coincidences was monitored. To act as heralds for their respective idler partner, the signal photons were split off via a PBS. The idler photons were also sent through a PBS to identify their polarization. Idler photons leaving from the V-polarized port of the Sagnac loop were rotated with a half-wave plate to become identical in polarization with the photons leaving from the H port. The photons are then interfered on a 50:50 beamsplitter. For maximal spatial overlap of idler photons at the 50:50 beamsplitter, there is a single-mode fiber between the grating and the first PBS in the Hong-Ou-Mandel setup. The degree of temporal overlap between the idler wavepackets was controlled by moving a retroreflector to adjust the path delay. The rate of four-fold coincidences is recorded against the position of this retroreflector.

The main source of noise in this measurement is multiple pair generation from a single pump pulse causing a background that reduces the visibility of the HOM interference. The background rate can be determined by sequentially blocking each input port of the 50:50 beamsplitter, and adding up the remaining four-fold coincidences. At 1 mW of pump power ($g^{(2)}(0) \approx 0.08$ and C/A ≈ 30), the average rate of four-fold coincidences was $\approx 0.03\,\mathrm{s}^{-1}$. These are comparable with some of the brightest four-fold coincidences reported via SPDC ($0.004\,\mathrm{s}^{-1}$ [31]) or SFWM ($0.04\,\mathrm{s}^{-1}$ [16]).

When the idler photon wavepackets had maximal spatial overlap, a dip was obtained in the raw four-fold coincidence rate with a visibility of $82 \pm 6\%$. When the estimated four-fold accidentals rate ($\approx 0.005\,\mathrm{s}^{-1}$) is subtracted, we find that the dip is compatible with unit visibility

(fig. 5(b)). This result indicates that by operating at lower pump power (but requiring longer integration times or higher repetition rates), it is possible to herald purely indistinguishable single photons.

5. Conclusion

We have reported on a substantial improvement in building brighter and more compact sources of single-mode photon-pairs using photonic crystal fibers. This improvement was brought about by the use of end-tapered PCFs and novel spectral filters. We studied the photon-pair emission characteristics of a pulse-pumped end-tapered PCF, and presented the dependence of count rates and noise on pump power.

It was observed that a relatively high photon-pair count rate ($3,800$ pairs s^{-1}) could be obtained with a low level of background noise ($g^{(2)}(0) = 0.03$). The combination of high count rate and low background noise makes it possible to build bright sources of high quality polarization-entangled photon-pairs by placing the PCF in a Sagnac loop. Another advantage of the bi-directionally pumped Sagnac loop is that a single PCF can act as *two* sources of heralded single photons, that are essentially indistinguishable. Our source is (spectrally) brighter while at the same time displaying better photon-purity, indistinguishability and polarization-entanglement quality compared to previous implementations of fiber-based photon-pair sources [14, 15, 16].

One direction of current research is to use PCFs [33, 34, 35] to generate factorizable states, which in principle, can remove the need for spectral filtering. In [35], a custom PCF was used to generate nearly factorizable states, allowing a four-fold rate of 0.3 s^{-1} to be achieved. The combination of factorizable states, end-tapers and mode-matching optics could lead to sources with even higher levels of detected pair brightness. Furthermore, PCFs in such arrangements need not be limited to photon-counting experiments since it is also possible to use end-tapered fibers to generate squeezed light [36, 37]. Together, these possibilities highlight the potential of end-tapered PCFs as a source of non-classical light.

6. Acknowledgments

This work has been supported in part by the Intelligence Advanced Research Projects Activity (IARPA) entangled photon source program.